Temperature sensitivity of soil organic carbon respiration along a forested elevational gradient on the Rwenzori Mountains, Uganda

Deleted: Mt.

Joseph Okello[1,2,3,4], Marijn Bauters[1,2], Hans Verbeeck[2], Samuel Bodé[1], John Kasenene[3], Astrid Françoys[1,5,6], Till Engelhardt[7], Klaus Butterbach-Bahl[8], Ralf Kiese[8] and Pascal Boeckx[1]

[1]Isotope Bioscience Laboratory – ISOFYS, Ghent University, Coupure Links 653, 9000 Gent, Belgium
[2]CAVElab- Computational and Applied Vegetation Ecology, Ghent University, Coupure Links 653, 9000 Gent, Belgium
[3]School of Agriculture and Environmental Sciences, Mountains of the Moon University, P.O Box 837, Fort Portal, Uganda
[4]National Agricultural Research Organisation, Mbarara Zonal Agricultural Research and Development Institute, P.O Box 389, Mbarara, Uganda
[5]Soil Fertility and Nutrient Management (SoFer), Ghent University, Coupure Links 653, 9000 Gent, Belgium
[6]Soil Physics (SoPHy), Ghent University, Coupure Links 653, 9000 Gent, Belgium.
[7]Sweco, Arenbergstraat 13, 1000 Brussels, Belgium
[8]Institute for Meteorology and Climate Research, Atmospheric Environmental Research (IMK-IFU), Karlsruhe Institute of Technology, Kreuzeckbahnstrasse 19, Garmisch-Partenkirchen 82467, Germany

Correspondence to: Joseph.Okello@UGent.be

Key words: Temperature sensitivity, CO_2 respiration, climate warming, Afromontane forests

Abstract

Tropical montane forests store high amounts of soil organic carbon (SOC). However, global warming may affect these stocks via enhanced soil respiration. Improved insight into the temperature response of SOC respiration can be obtained from *in* and *ex situ* warming studies. *In situ* warming via translocation of intact soil mesocosms was carried out along an elevational gradient ranging between ca. 1250 m in the Kibale Forest to ca. 3000 m in the Rwenzori Mountains in Uganda. Samples from the same transect were also warmed *ex situ*. *Ex situ* results revealed that following the elevational gradient which represents a natural climate gradient, specific heterotrophic CO_2 respiration decreased linearly by 1.01 ± 0.12 µg C h^{-1} g^{-1} SOC per 100 m of elevation increase. The coefficient of temperature sensitivity increased from 1.50 ± 0.13 in the lowest to 2.68 ± 0.25 in the highest elevation cluster, showing a linear increase of 0.09 ± 0.03 per 100 m of elevation increase. Additionally, respired CO_2 was more depleted in ^{13}C in the warmer lower elevations as compared to colder higher elevations, with a linear decrease of 0.23 ± 0.04 ‰ per 100 m of elevation increase. Furthermore, microbial community structure indicated a weak trend along the elevational gradient with higher elevations more dominated by fungi relative to bacteria. The results indicate an increased recalcitrance and decreased mineralisation of SOC with elevation likely driven by decreasing soil temperature and pH. Subsequently, after two years of *in situ* warming (0.9 to 2.8 °C), specific heterotrophic SOC respiration tended to be lower for warmed as compared to control soil. Further, in warmed soils, $\delta^{13}C$ values and SOC content respectively increased and decreased. Collectively, this points towards increased mineralisation and depletion of readily available C during two years of warming. In conclusion, our results suggest that climate warming may trigger enhanced losses of SOC from tropical montane forests, due to a combination of a higher temperature sensitivity of mineralisation and higher SOC content at higher elevations.

Deleted: soil organic carbon

Deleted: soil organic carbon

Deleted: a.s.l.

Deleted: a.s.l.

Deleted: elevation clusters

Deleted: depletion factor of the respired CO_2 decreased

Deleted: ly by

Deleted: soil organic carbon

Deleted: soil organic carbon

Deleted: s

Deleted: , respectively

Deleted: carbon

Deleted: soil organic carbon

Deleted: soil organic carbon

1 Introduction

Tropical forests store 55 % of the global forest carbon (C) stocks of which 56 % is stored in biomass, 32 % in soil and 12 % in litter and deadwood (Pan et al., 2011). These forests account for more than one-third of primary productivity (Beer et al., 2010; Pan et al., 2011), despite covering only less than 10 % of the global land area (Cuni Sanchez et al., 2021; Erb et al., 2018). Their key role in the global C cycle is further demonstrated by the fact that tropical forests exchange more carbon dioxide (CO_2) with the atmosphere than any other ecosystem (Friedlingstein et al., 2020; Lewis et al., 2015; Singh, 2018), in part owing to their high C turnover rates (Sayer et al., 2011). Currently, tropical ecosystems are being subjected to global change, with detrimental consequences for its ecosystem services (Gütlein et al., 2018). The global temperature increase is being driven by global climate warming and local land use change (Friedlingstein et al., 2020; Zhang et al., 2005; Ipcc, 2018). For instance, worldwide, the average surface temperature has been rising consistently by 0.95-1.20 °C from 1850 to 2020 (IPCC, 2021). In addition to the global climate warming effect, tropical forests are also experiencing local and regional temperature increases driven by land use change, which alters the fluxes of solar and thermal infrared radiation, sensible, and latent heat and ultimately changes the surface albedo (Mahmood et al., 2014; Zeng et al., 2021). As an example, between the year 2000 and 2014, agricultural expansion at the expense of montane forests caused a general increase in air temperature of 0.05 ± 0.01 °C in the Albertine rift mountains of Africa, and air warming of up to 2 °C can occur under extensive deforestation (Zeng et al., 2021). The increase in global and regional temperature has the potential to drastically alter the C cycle in tropical forests (Mohan, 2019; Nottingham et al., 2020; Sayer et al., 2019), and may potentially drive accelerated soil organic C (SOC) losses (Friedlingstein et al., 2020; Kim et al., 2016). However, the response of tropical forest soils to such temperature increases is largely uncertain, especially in mountainous areas (Nottingham et al., 2020; Sayer et al., 2019; Zeng et al., 2021), and generally data on climate warming from tropical forests in Africa are hardly available.

Deleted: between

Key in this ecosystem-level uncertainty, is the specific effect of warming on soil respiration rates (Carey et al., 2016; Crowther et al., 2016; Fussmann et al., 2014). Indeed, up to about 40 % of the CO_2 emissions from tropical forest ecosystems originate from soil respiration (both autotrophic and heterotrophic respiration) (Malhi, 2012), of which approximately 60 % of the CO_2 respiration from soil is derived from heterotrophic microbial activity during the mineralisation of organic C (Sayer and Tanner, 2010). Temperature increases in tropical forests can trigger accelerated respiration rates, yet the ecosystems' net primary productivity is already close to its maximum, thereby reducing the net C sink (Carey et al., 2016; Craine et al., 2010; Nottingham et al., 2020). Therefore, given the sheer magnitude of both the C storage and emission capacities of tropical forest soils, precise quantifications and assessment of their response to climate warming are needed to inspire climate-sensitive forest management and to improve parameterisation and predictions of earth system models (Oertel et al., 2016; Quéré et al., 2018).

Several short-term warming studies indicated increased soil microbial respiration with increase in temperature (Karhu et al., 2014; Nazaries et al., 2015). Contrastingly, others reported microbial acclimatization to warming (Bradford et al., 2008; Luo

et al., 2001). Here we present new data from an eastern Afrotropical elevational gradient set up in the Kibale Forest and the Rwenzori Mountains in western Uganda. We studied the diffusive flux of CO_2 from soil incubations and used it as a close proxy for microbial respiration (hereafter referred to as "CO_2 respiration"). To gain better insight into the drivers of SOC respiration, in function of elevation and enhanced warming, we investigated: (i) soil physicochemical properties and the microbial community compositions based on phospholipid fatty acid analysis (PLFA), (ii) heterotrophic soil CO_2 respiration rate from laboratory incubations at 60 % water-filled pore space (WFPS) and controlled corresponding *in situ* temperature, (iii) changes in heterotrophic soil CO_2 respiration from intact mesocosm translocated *in situ* along an elevational gradient to simulate a warming of about 2°C, (iv) activation energies (AE) and temperature sensitivities (Q_{10}) of heterotrophic soil CO_2 respiration rates and finally, (v) seasonal total soil CO_2 respiration rate under *in situ* conditions. In particular, we intend to address the following research questions, with respect to a tropical Afromontane elevational gradient

i. Does soil organic matter recalcitrance increase with elevation?
ii. How does SOC respiration respond to two years of *in situ* soil warming?

Deleted: transect
Deleted: soil organic C (
Deleted:)
Deleted: transect
Deleted: soil organic carbon

2 Materials and Methods

2.1 Study area

The study was conducted in the Kibale Forest National Park and the Rwenzori Mountains National Park in Uganda, both protected by the Uganda Wildlife Authority. A total of twenty sampling plots, each measuring 40 m by 40 m, were established between 1250 to 3000 m along an elevational gradient (all elevations refer to above sea level (a.s.l.). The sampling plots were grouped into five elevation clusters, with each cluster consisting of four replicated plots within similar elevations and environmental conditions. From the twenty sampling plots, four plots are located in the Kibale Forest National Park at an elevation of 1250-1300 m to form the "premontane" elevation cluster. Sixteen sample plots are located at four different elevation clusters (1750-1850, 2100-2200, 2500-2600 and 2700-3000 m) in the eastern slope of the Rwenzori Mountains National Park (Figure 1).

Deleted: eters
Deleted: above sea level (m a.s.l.)
Deleted: a.s.l.
Deleted: a.s.l.
Deleted: Figure 1

The Kibale Forest National Park (795 km²; 00°30'N 30°24'E) is located in the Kabarole and Kamwenge districts of western Uganda. The climate is moist tropical, and temperatures stay nearly constant all-year-round. The average annual rainfall is 1365 ± 53 mm and the average temperature is 27.8 ± 0.74 °C (data 1992-2012, Kyembogo weather station in Kabarole district 20 km from the park, at elevation of 1400 m, Ministry of Water and Environment). The dominant soil type according to the World Reference Base (WRB) classification is Ferralsol (Jacobs et al., 2016).

Deleted: a.s.l.

The Rwenzori Mountains National Park (998 km^2; between 0°06'S – 0°46'N and 29°47'E – 30°11'E) is located at the border between the Democratic Republic of the Congo (DRC) and Uganda. The region experiences a moist tropical climate, locally

affected by altitude and topography. Annual rainfall varies with elevation and slope aspect, with the highest rainfall amounts on the eastern slope, where our transect was established. Recent rainfall data from the Uganda Wildlife Authority from 2012 to 2015 showed variations in mean annual rainfall ranging from 1570 ± 334 mm at 1760 m to 1806 ± 322 mm at 4230 m. The mean annual soil temperature of the different elevation clusters is indicated in Figure 1. The dominant soil type in the Rwenzori Mountains according to WRB classification is Leptosol (Jacobs et al., 2016).

Deleted: 7000
Deleted: a.s.l.
Deleted: 570
Deleted: a.s.l
Deleted: .

2.2 Soil physicochemical properties and microbial community structure

In each study plot, the soil temperature at 5 cm depth was measured daily (during the measurements of soil respiration) at an interval of 30 minutes, using thermocron iButton sensors DS1921G-F5 (iButton, Thermocron Baulkham Hills, Australia). Similarly, the daily volumetric soil moisture content was measured at 5 cm soil depth using soil moisture sensors (EC-5, Decagon Devices, Armidale, Australia). Further, soil bulk density was determined using the soil core method (Campbell and Henshall, 2000).

At each of the twenty sampling plots along the elevational gradient, four topsoil samples (0-10 cm) of 385 cm^3 by volume were collected (i.e. one sample per 20 m by 20 m subplot within the 40 by 40 m sample plot) and homogenised to form one composite sample per plot (4 replicate composite samples per elevation cluster). The samples were oven-dried at 60 °C and sieved through 2 mm mesh size and ground. Subsequently, C, nitrogen (N) content and respective $\delta^{13}C$ and $\delta^{15}N$ values were determined from the composite soil samples using an elemental analyser (automated nitrogen carbon analyser; ANCA-SL, SerCon, Cheshire, U.K.), coupled to an isotope ratios mass spectrometer (IRMS; 20-22, SerCon, Cheshire, U.K.). The measured C was considered as SOC because in acidic soils of the wet tropics, the presence of carbonates is negligible. For measurement of $\delta^{13}C$ values, the standard used was VPDB (Vee Pee Dee Belemnite), while $\delta^{15}N$ values were measured in reference to air. To measure the soil pH, 5 mL of the oven-dried soil (in triplicate) was brought into suspension with 25 ml of 1*M* KCl (1:5 v/v) and shaken end-over-end for one hour. Subsequently the suspension was left to settle for two hours, then soil pH was measured in the supernatant using a pH glass electrode, (model 920A, Orion, England).

Deleted: transect

For determination of the microbial community structure, about 20 g of the homogenised composite sample from each plot was frozen immediately after collection. The microbial community structure was determined using phospholipid fatty acid (PLFA) analysis. The PLFA analysis was done by extracting 5 g of freeze-dried soil sample in duplicate following the method described by Bligh and Dyer (1959), and as modified by Findlay et al. (1989). Briefly, the method involves extraction of all fatty acids, followed by isolation of phospholipids from other soil lipids (using solid-phase extraction), and finally the conversion into fatty acid methyl esters. Accordingly, for each gram of soil sample, lipid extraction was done using a combination of 0.1*M* phosphate-buffer, trichloromethane and methanol solvents (0.9:1:2, v/v) at 25°C. Subsequently, the volume of the total lipid extracts was reduced by evaporating the solvent from tubes under N gas in a water bath at 30 °C. After, the neutral lipids and

glycolipids were eluded using trichloromethane and acetone respectively. Phospholipids were further eluded using methanol and concentrated by evaporation of the solvent under N gas in a water bath at 30 °C. Eventually, the phospholipid fatty acids were converted to methyl esters, which were subsequently analysed using gas chromatography (GC, Trace GC, Thermo Scientific, Bremen, Germany), following the methods described by Denef et al. (2007) and Huygens et al. (2011). We determined the ratios of the peak area of each individual PLFA to that of C16:0, a universal PLFA occurring in the membranes of all organisms. PLFA ratios less than 0.02 were excluded from the data set (Drijber et al., 2000). PLFA was assigned to a fungal group following Zelles, (1997), and Chung et al., (2007), while PLFA assignment to a bacterial group and to gram-positive and gram negative bacteria followed the procedure described by Kroppenstedt (1985) and Frostegård and Bååth (1996).

Deleted: .

2.3 Laboratory incubations

To assess soil heterotrophic CO_2 respiration rates under controlled laboratory incubations, the homogenised composite samples from each plot were air-dried and sieved (2 mm mesh size) to remove coarse particles and roots. For the incubation experiments, 50 g of each air-dried composite soil sample from each plot (4 replicates per elevation cluster) was placed in a gas jar of 1 L, which could be closed in an air-tight way by a lid. To each sample, deionised water was added until 60 % WFPS of the respective soil sample (based on total porosity derived from bulk density measurements), representing a moisture content for optimal microbial activity (Aon et al., 2001; Doetterl et al., 2015). The samples were then pre-incubated for 14 days (at the respective *in situ* mean annual temperature per elevation cluster, i.e., 20, 17, 15, 13 and 12 °C for elevation clusters of 1250-1300, 1750-1850, 2100-2200, 2500-2600 and 2700-3000 m respectively). These temperatures were controlled by placing the jars in incubators with the respective temperatures. During the pre-incubation, the gas jars were closed with parafilm to permit free air circulation while minimizing the loss of water.

Deleted: ,

Deleted: a.s.l.

After 14 days of pre-incubation, each sample was removed from the incubator and flushed for 10 seconds with ambient air in the room by means of an air fan. Immediately, one gas sample was taken using a 45 mL syringe and the ambient CO_2 concentrations, and $\delta^{13}C$ values of ambient CO_2 at "open conditions" analysed using Cavity Ring-Down Spectrometer, (G2113-I, CRDS CO_2 analyser, Picarro, United States) at starting condition. The jars were then closed and placed back in the incubators for 24 hours (a preliminary trial experiment indicated a continuous linear increase in headspace CO_2 concentrations during 24 hours). After 24 hours, a 45 mL gas sample was taken and was immediately introduced into the cavity ring-down spectrometer for measurement of the CO_2 concentration and $\delta^{13}C$ values of the respired CO_2. After collecting the gas samples under closed conditions, the jars were opened, soil moisture replenished to 60 % WFPS, after which the jars were covered with parafilm and placed back in the incubator until the following measurement (to avoid gas accumulation and to re-establish ambient CO_2 concentrations). The following day, the same procedure was repeated, and this was done for five consecutive

Deleted: isotopic composition

Deleted: isotopic composition

days to attain five replicated CO_2 concentrations that were used to calculate the average respiration rate. To determine the $\delta^{13}C$ values of the respired CO_2, we used a mass balance approach (Phillips and Gregg, 2001) (equation 1).

$$\Delta^{13}C\text{-}CO_2 \approx \frac{[CO_2]_{final} * \delta^{13}C\text{-}CO_{2final} - [CO_2]_{initial} * \delta^{13}C\text{-}CO_{2initial}}{[CO_2]_{final} - [CO_2]_{initial}} \quad (1)$$

Where:

$[CO_2]_{final}$ = final concentration of CO_2 in the headspace;

$\Delta^{13}C\text{-}CO_{2final}$ = final $\delta^{13}C$ of CO_2 in the headspace;

$[CO_2]_{initial}$ = initial concentration of CO_2 in the headspace;

$\delta^{13}C\text{-}CO_{2initial}$ = initial $\delta^{13}C$ of CO_2 in the headspace.

Subsequently, the isotopic fractionation, epsilon (ε), i.e. the extent to which the product of respiration (i.e. CO_2) becomes depleted or enriched in ^{13}C during SOC (substrate) respiration was determined using equation 2.

$$\varepsilon = \left(\left(\frac{\text{R-}CO_2}{\text{R-SOC}}\right) - 1\right) * 1000 \quad (2)$$

Where:

ε is the isotopic fractionation

R-CO_2 is the ratio of ^{13}C to ^{12}C of the emitted CO_2

R-SOC is the ratio of ^{13}C to ^{12}C of soil organic carbon (substrate).

2.4 Long-term *in situ* warming: soil mesocosm translocation along an elevational gradient

In situ climate warming was simulated by translocating intact soil cores (16 cm diameter and 25 cm depth increment) along the altitudinal gradient to the nearest elevation cluster downslope (Figure 1). These intact soil cores were taken using a metallic soil corer in which a plastic PVC tube was inserted to collect an intact soil mesocosm. From each plot, four soil mesocosms were translocated downslope (hereafter referred as "warmed"), while four mesocosms were transplanted within the same plot (hereafter referred as "control"). Each elevation cluster (except the highest) therefore had a total of 16 warmed and 16 control soil mesocosms. The soil mesocosms that were translocated from higher to lower elevation clusters were warmed by about 0.9 to 2.8 °C on average for two years (Figure 1).

Deleted: the

Deleted: Keeling mass balance approach (Keeling, 1958)

Deleted: F = final concentration of CO_2 in the headspace;¶
f = final $\delta^{13}C$ of CO_2 in the headspace; ¶
I = initial concentration of CO_2 in the headspace;¶
i = initial $\delta^{13}C$ of CO_2 in the headspace.¶

Deleted: depletion factor

Deleted: $\varepsilon = \left(\left(\frac{1000 + \delta^{13}C\text{-SOC}}{1000 + \delta^{13}C\text{-}CO_2}\right) - 1\right) * 1000$

Deleted: depletion factor

Deleted: $\delta^{13}C$-SOC is the $\delta^{13}C$ of the soil organic carbon¶

Formatted: Indent: Left: 0"

Deleted: $\delta^{13}C\text{-}CO_2$ is the $\delta^{13}C$ of the respired CO_2.¶
The component $\left(\frac{1000 + \delta^{13}C\text{-SOC}}{1000 + \delta^{13}C\text{-}CO_2}\right)$ is alpha (α), which is the isotopic fractionation factor.¶

Deleted: transect

Deleted: Figure 1

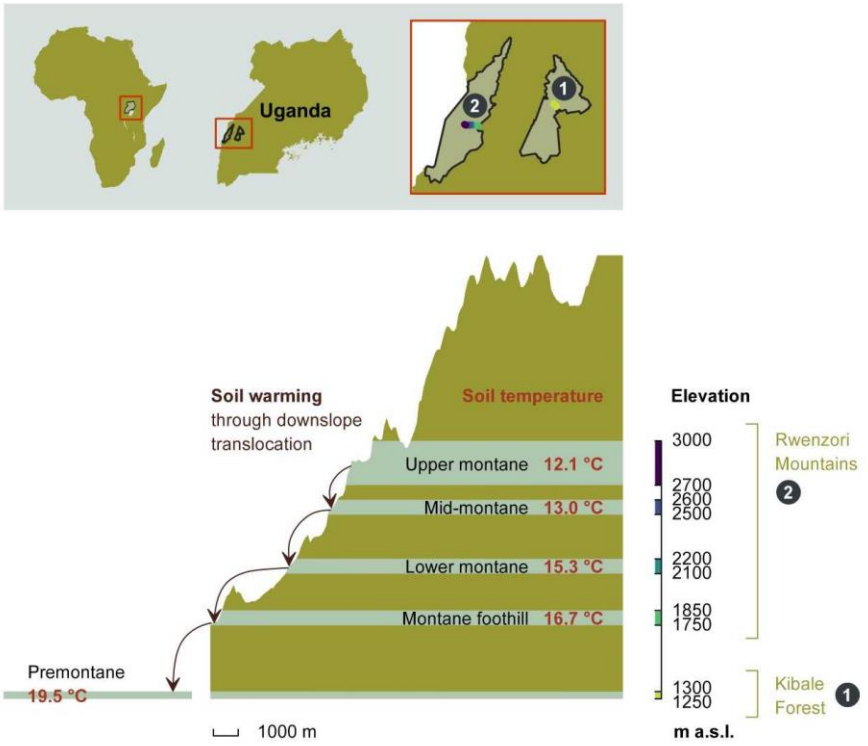

Figure 1. The height profile of the Rwenzori elevational gradient starting from nearby premontane Kibale Forest National Park (1250-1300 m a.s.l.) onto the Rwenzori Mountains National Park (1750-3000 m a.s.l.). Mean annual *in situ* temperatures for each of the five elevation clusters are indicated. The set-up of *in situ* warming through downslope translocation of soil cores to the immediate lower elevation cluster is illustrated on the left side of the scheme. Different colours on the elevation axis represent the colour code for each elevation cluster throughout the manuscript.

After 650 days of *in situ* incubation between November 2017 to September 2019 of both control and warmed soil cores, the cores were collected. The top 10 cm of the soil cores was collected (i.e. the soil layer with the highest C content and most active in C cycling), homogenised, air-dried, and sieved (2 mm mesh size) for additional laboratory incubation experiments, in order to assess the effect of two years of *in situ* warming on: (i) CO_2 respiration rates, (ii) the AE and Q_{10} coefficient, (iii) SOC content and soil $\delta^{13}C$ values.

To assess the above parameters (i-iii), the soil samples from the translocation experiment were subjected to another incubation experiment under optimal soil moisture conditions. Firstly, the control and warmed samples were incubated at the corresponding mean annual soil temperatures at which they were transplanted *in situ* (Table 1). Additionally, subsamples from the same soil were also incubated at four other temperatures (5, 10, 15 and 30 °C, covering the temperature ranges in the entire elevational gradient) to allow determination of AE and Q_{10} through curve fitting of the CO_2 respiration rates at five different temperatures.

For these experiments, 6-15 g of air-dried soil (where the mass depended on the bulk density) was placed in the gas jar (50 mL by volume) for each temperature treatment and moistened with deionised water to attain 60 % WFPS. The soil was then gently compressed to a pre-determined height in correspondence with the bulk density of the undisturbed soil. Subsequently, the jars were weighted, covered with parafilm and pre-incubated for 14 days to allow for the re-activation and stabilisation of microbial activities. During the pre-incubation, the soil moisture content in each jar was monitored, and when needed corrected by adding deionised water. After 14 days of pre-incubation, the collection of air samples for the determination of CO_2 respiration rate was initiated by removing the parafilm, aerating the samples and closing the lids in an air-tight way. The CO_2 concentrations at starting condition and after 24 hours were analysed using a gas chromatograph (Finnigan Trace GC Ultra, Thermo Electron Corporation, Milan, Italy) fitted with a thermal conductivity detector. Eventually, the CO_2 respiration rate was determined as the change in headspace CO_2 concentrations divided by the incubation time (ca. 24 hours).

2.5 *In situ* total soil CO_2 respiration

Along the Rwenzori elevational gradient, we selected one sampling plot in each of the four elevation clusters at 1250-1300, 1750-1850, 2100-2200 and 2700-3000 m, for the collection of *in situ* gas samples. In each study plot, *in situ* total soil respiration rates were measured following the static chamber method (Collier et al., 2014). Each sampling plot was subdivided into four 20 m by 20 m subplots. In each plot, five positions for static chambers were identified, with one position per 20 m by 20 m subplot, and another one in the center of the 40 m by 40 m permanent sample plot. The collars of the static chambers (to anchor the chamber in the soil) were installed in the soil at least 24 hours before the first gas sampling event and were maintained in the field throughout the sample collection periods to minimise the effect of soil disturbance. The depth of the installed collar was noted for precise volume correction of the headspace. Natural litter cover was left intact but plants were

Deleted: isotopic composition

Deleted: transect

Deleted: slope of CO_2 concentration in function of time.

Deleted: transect

Deleted: a.s.l.

not included within the measuring chamber. For respiration rate measurements a static, opaque gas chamber was placed on top of the collar, to create a headspace in which CO_2 emitted from the soil can accumulate. Both the collars and the chambers are made of polyvinylchloride (PVC) material and were painted white to limit heating of the chamber's headspace air. The chamber was equipped with a vent tube to minimise pressure differences, and a septum connected to a three-way valve to allow the collection of headspace air samples. The headspace volume of the static gas chamber was 4 L and the surface area was 0.019 m^2. The set up ensured that the conditions for a non-steady state closed chamber flux measurements were still respected.

Deleted: 5

During each sampling event, the five gas chambers were closed for 90 minutes, during which 15 mL air samples were collected with a syringe from the chamber headspace at 30-minute intervals starting at time 0 minute until 90 minutes (i.e. $t_1 = 0$, $t_2 = 30$, $t_3 = 60$, and $t_4 = 90$ minutes). Prior to air sample collection, the gas chamber headspace was flushed three times with its headspace air using the sampling syringe to homogenise the air in the gas chamber headspace. Headspace air samples of 15 mL each were immediately injected in 12 mL pre-evacuated air-tight vials (Labco, Lampeter, Wales, U.K) that were closed with a silicone septum (Dow Corning 734). This created a slight over-pressure in the vials. The headspace air samples were collected for five consecutive days during the start of the rainy season (August 2019), and the same process was repeated in the mid rainy season (September 2019) to account for any seasonal variations in environmental conditions. CO_2 emission measurements were not done in the dry season because microbial respiration and temperature sensitivity are low when the WFPS is below 30 % (Aon et al., 2001). The collection of headspace air samples was always consistently executed between 11:00 and 13:00 hours in all plots to minimize the effect of diurnal temperature differences (Keane and Ineson, 2017). The linearity of the headspace CO_2 concentration increases over the full 90 minutes were checked and always fulfilled.

2.6 Determination of CO_2 respiration rates, AE and Q_{10}

To convert the measured CO_2 concentrations into respiration rates, we fitted a linear regression of the concentrations over time (for *in situ* measurements) or determined the change in headspace CO_2 concentrations divided by incubation time (for laboratory incubation measurements). The derived soil CO_2 respiration rates were then expressed in units of grams of C per unit area per hour (for *in situ* measurements) or units of grams of C per unit of soil per hour or normalised per unit SOC (for laboratory incubations) to obtain the "specific" heterotrophic CO_2 respiration rate. This was done using the ideal gas law as described in equation (3) to obtain the net gas respiration rates taking into account the headspace volume of the gas chamber, pressure, temperature and molar weight of the gas (Collier et al., 2014; Dalal et al., 2008; Kutzbach et al., 2007).

$$F_C = \left[\frac{\Delta C}{\Delta t}\right] * \left[\frac{P*V}{R*T*A}\right] * M_w \quad (3)$$

Where:

F_C is the resulting gas respiration rate in (g C m^{-2} h^{-1}) (for *in situ* respiration rates)

ΔC is the change in gas concentrations (ppm)

Δt is the change in incubation time (hour)

P is the pressure (atm)

V is the volume of the gas chamber headspace (L)

R is the molar gas constant (L atm mol^{-1} K^{-1})

T is the absolute temperature (K)

A is the surface area of the gas chamber (m^2)

M_w is the molar weight (g mol^{-1})

For the laboratory incubation experiments, the parameter A (i.e. the surface area of the gas chamber) was replaced either by the weight of the incubated soil (to express it as "mg C h^{-1} kg^{-1} soil" or by the amount of soil SOC (to express it as "µg C h^{-1} g^{-1} SOC").

Deleted: concentration

To determine the activation energy of CO_2 respiration rate, we employed equation (4) with the respiration rate expressed per unit SOC.

$$F_C = b * e^{\frac{-AE}{R*T}} \quad (4)$$

Where:

F_C is the specific CO_2 respiration rate (µg C h^{-1} g^{-1} SOC)

b is a pre-exponential factor (that is, the theoretical reaction rate constant in the absence of activation energy)

AE is the activation energy in kJ mol^{-1}

After log transformation, equation (4) becomes:

$$\ln F_C = AE * \left[\frac{-1}{R * T}\right] + \ln b \quad (5)$$

Hence, when plotting $\ln F_C$ against $\frac{-1}{R*T}$, the activation energy can be determined as the slope of the linear regression (SI Figure 1).

Deleted: SI,

To determine the coefficient for temperature sensitivity of SOC respiration (Q_{10}), the CO_2 respiration at five different incubation temperatures were firstly fitted to an exponential function, i.e. equation (6) (SI Figure 2).

Deleted: SI,

$$F_C = a * e^{k*T} \quad (6)$$

From the two exponential regression constants a and k, the k value was used to calculate the Q_{10}, using equation (7).

$$Q_{10} = e^{10*k} \quad (7)$$

350

2.7 Data Analysis

To determine whether there was a difference in the CO_2 respiration rates, AE and Q_{10} among the elevation clusters in the elevational gradient, we employed analysis of variance (ANOVA) to check differences in means of each variable. Where a significant difference was detected, post-hoc analysis for multiple comparisons was performed using Tukey honest comparison 355 of means to explicitly reveal which elevation clusters differed from each other. We used quantile-quantile and residual plots to check whether the data followed assumptions of ANOVA. To check whether there was a dependency of CO_2 respiration rates, AE and Q_{10} on elevation, we used the linear mixed effect model regression "lme4" package in R software, in which elevation was used as fixed effect and elevation cluster location as random effect (to control for spatial clustering of the sampling plots). To estimate the *P*-values, we used type III analysis of variance with Satterthwaite's approximation method in 360 the linear mixed effect model. In each linear mixed effect model, both marginal R square (R^2_m) and conditional R square (R^2_c) values were obtained following Nakagawa and Schielzeth (2013). Further, to check for a change in CO_2 respiration rates, AE, Q_{10}, SOC content and $\delta^{13}C$ values between control and *in situ* warmed soil at each elevation cluster, we used a Wilcoxon test. Subsequently, to check the effect of warming along the entire elevational gradient, we fitted linear mixed effect model for both control and warmed soil, where elevation was used as fixed effect and the elevation clusters as random. Finally, we employed 365 principal component analysis to explore changes in microbial community and soil physicochemical properties along the elevational gradient. All data were analysed using R software (R Core Team, 2021), and a *P*-value of 0.05 was taken as significance level.

Deleted: transect

Deleted: isotopic composition

Deleted: transect

Deleted: transect

3 Results

3.1 Physicochemical soil properties and microbial community

The physicochemical soil properties in the Rwenzori elevational gradient are described in Table 1. Along the elevational gradient, average annual soil temperature, bulk density and pH_{KCl} decreased linearly. On the other hand, SOC, soil total N and carbon-to-nitrogen (C:N) ratio, increased linearly with increasing elevation. Further, the $\delta^{13}C$ values of the SOC showed no linear trend along the elevational gradient.

Deleted: transect

Deleted: On the other hand

Deleted: .

Table 1. Physicochemical soil properties (0-10 cm) of the elevational gradient on the east-facing slope of the Rwenzori Mountains National Park (1750-3000 m a.s.l.) and the premontane Kibale Forest National Park (1250-1300 m a.s.l.). Indicated are the mean values plus/minus standard deviations of average annual soil temperature at 5 cm depth, bulk density (ρ_b), pH in KCl solution (pH_{KCl}), soil organic carbon (SOC) content, total nitrogen (TN) content, carbon-to-nitrogen ratio (C:N), , $\delta^{13}C$ values and $\delta^{15}N$. The elevational trend from the linear mixed effect regression model estimate per 100 m of elevation increase is also indicated with the standard error (SE), *P*-value, marginal R^2 (R^2_m) and conditional R^2 (R^2_c).

Elevation cluster (m a.s.l.)	1250-1300	1750-1850	2100-2200	2500-2600	2700-3000	Fixed effect estimate per 100 m	SE	*P*-value	R^2_m	R^2_c
Soil class	Ferralsol	Leptosol	Leptosol	Leptosol	Leptosol	NA				
Soil temperature (°C)	19.5 ± 1.1[a]	16.7 ± 0.8[b]	15.3 ± 1.0[c]	13.0 ± 0.9[d]	12.1 ± 1.1[e]	-0.51	0.00	<0.001*	0.90	0.90
ρ_b (g cm^{-3})	1.04 ± 0.09[a]	0.77 ± 0.13[b]	0.51 ± 0.07[c]	0.45 ± 0.07[c]	0.44 ± 0.08[c]	-0.04	0.00	0.009*	0.78	0.85
pH_{KCl}	5.41 ± 0.29[a]	4.13 ± 0.11[b]	4.00 ± 0.13[b]	3.56 ± 0.13[c]	3.25 ± 0.21[c]	-0.13	0.02	0.011*	0.83	0.91
SOC (%)	4.04 ± 1.41[c]	5.31 ± 2.15[c]	13.36 ± 0.68[b]	18.27 ± 3.58[a]	22.97 ± 4.29[a]	1.33	0.22	0.007*	0.81	0.89

TN (%)	0.44 ± 0.12^{c}	0.60 ± 0.24^{c}	1.09 ± 0.17^{b}	1.40 ± 0.20^{ab}	1.81 ± 0.25^{a}	0.09	0.01	0.006*	0.82	0.87
C:N	9.1 ± 0.7^{b}	8.9 ± 0.5^{b}	12.5 ± 1.6^{a}	13.0 ± 0.7^{a}	12.6 ± 0.9^{a}	0.31	0.09	0.041*	0.59	0.82
$\delta^{13}C$ (‰)	-25.5 ± 0.6^{ab}	-24.5 ± 0.9^{a}	-25.3 ± 0.6^{ab}	-25.8 ± 0.7^{ab}	-26.4 ± 0.3^{c}	-0.06	0.05	0.345	0.13	0.51
$\delta^{15}N$ (‰)	6.07 ± 0.23^{a}	3.53 ± 0.49^{b}	-0.21 ± 0.54^{c}	-0.40 ± 0.23^{c}	-0.80 ± 0.30^{c}	-0.39	0.064	0.007**	0.83	0.93

Different lowercase letters in superscript (bold) next to values of each elevation cluster (same row) indicate a significant difference among the sites at $P < 0.05$. The mean values were calculated from 4 separate composite soil samples per elevation cluster and are expressed per unit of dry soil. The *P*-values for a statistically significant elevational linear trends are marked with an asterisk symbol "*". For measurement of $\delta^{13}C$ values, the standard used was VPDB (Vee Pee Dee Belemnite), while $\delta^{15}N$ values were measured in reference to air.

Further, at the start of the rainy season, the average *in situ* soil temperature at 5 cm depth decreased from 19.6 ± 0.3 °C at 1250-1300 m to 11.9 ± 0.5 °C at 2700-3000 m (SI Table 3). Generally, along the elevational gradient, the average soil temperature at the start of the rainy season decreased linearly at a rate of 0.50 ± 0.04 °C per 100 m of elevation increase (R^2_m = 0.96, *P* = 0.006, SI Figure 3). On the other hand, in the mid rainy season, the average *in situ* soil temperature decreased from 20.4 ± 0.4 °C at 1250-1300 m to 12.3 ± 0.4 °C at 2700-3000 m. Similarly, in the mid rainy season, the soil temperature decreased linearly by 0.52 ± 0.06 °C per 100 m of elevation increase (R^2_m = 0.92, *P* = 0.014, SI Figure 3). Additionally, at each elevation cluster, the average soil temperature at 5 cm depth was significantly higher in the mid rainy season than at the start of the rainy season (SI Table 3, SI Figure 3).

In addition, at the start of the rainy season, the average percentage WFPS was 33.1 ± 1.2 % at 1250-1300 m, 22.2 ± 2.5 % at 1750-1850 m, 41.7 ± 2.9 % at 2100-2200 m, and 42.7 ± 8.7 % at 2700-3000 m, (SI Table 3). Generally, along the elevational gradient, the average WFPS showed no significant elevational trend at the start of the rainy season (SI Figure 3). In the mid rainy season, the average percentage water-filled pore space was 57.2 ± 5.8 % at 1250-1300 m, 44.8 ± 3.8 % at 1750-1850 m, 45.4 ± 4.8 % at 2100-2200 m, and finally 44.5 ± 9.0 % at the highest elevation cluster (2700-3000 m) (SI Table 3). Generally, along the elevational gradient, the average WFPS showed no significant elevational trend in the mid rainy season (SI Figure 3). On the other hand, the soil moisture content was always higher in the mid rainy season in all elevation clusters except at 2700-3000 m (no significant difference) (SI Table 3).

Finally, along the elevational gradient, the microbial community composition showed no significant trend (SI Figure 4). The percentage of the variability explained by elevation was low for each microbial group, i.e. gram-positive bacteria (R_m^2 = 0.07), gram negative bacteria (R_m^2 = 0.01), fungi (R_m^2 = 012), total PLFA (bacteria plus fungi) (R_m^2 = 0.06), the ratio of gram-positive to gram-negative bacteria (R_m^2 = 0.05) and the ratio of bacteria to fungi (R_m^2 = 0.10) (SI Figure 4). Subsequently, the principle component analysis (PCA) of soil parameters (including microbial community composition), further confirmed that the ratio of bacteria to fungi depicted a weak negative correlation with elevation. Further, the ratio of gram-positive to gram-negative bacteria revealed a weak positive correlation with elevation (Figure 4, SI Table 2). The parameters of principle component 1 with correlation scores above 0.5 included the total PLFA (bacteria plus fungi), fungi, gram-positive and gram-negative bacteria and physicochemical soil properties (soil bulk density, temperature, pH, SOC, total N, C:N). On the other hand, parameters of principle component 2 included the total PLFA (bacteria plus fungi), fungi, gram-positive and gram-negative bacteria, and the ratio of gram-positive to gram-negative bacteria and soil pH. Generally, the PCA indeed revealed that the five elevation clusters have similar soil physicochemical properties. Further, it shows that the microbial community vectors are roughly orthogonal to the vectors of soil physicochemical properties. Up to 57.0 % and 23.3 % of the variability in the parameters were explained by principle component 1 and 2, respectively (Figure 2, SI Table 2).

Deleted: a.s.l.
Deleted: a.s.l.
Deleted: SI,
Deleted: transect
Deleted: SI,
Deleted: a.s.l.
Deleted: a.s.l.
Deleted: SI,
Deleted: SI,
Deleted: SI,
Deleted: a.s.l.
Deleted: a.s.l.
Deleted: a.s.l.
Deleted: a.s.l
Deleted: SI,
Deleted: transect
Deleted: SI,
Deleted: a.s.l.
Deleted: a.s.l.
Deleted: a.s.l.
Deleted: a.s.l.
Deleted: SI,
Deleted: transect
Deleted: SI,
Deleted: a.s.l.
Deleted: SI,
Deleted: transect
Deleted: SI,
Deleted: SI,
Deleted: SI,
Deleted: SI,

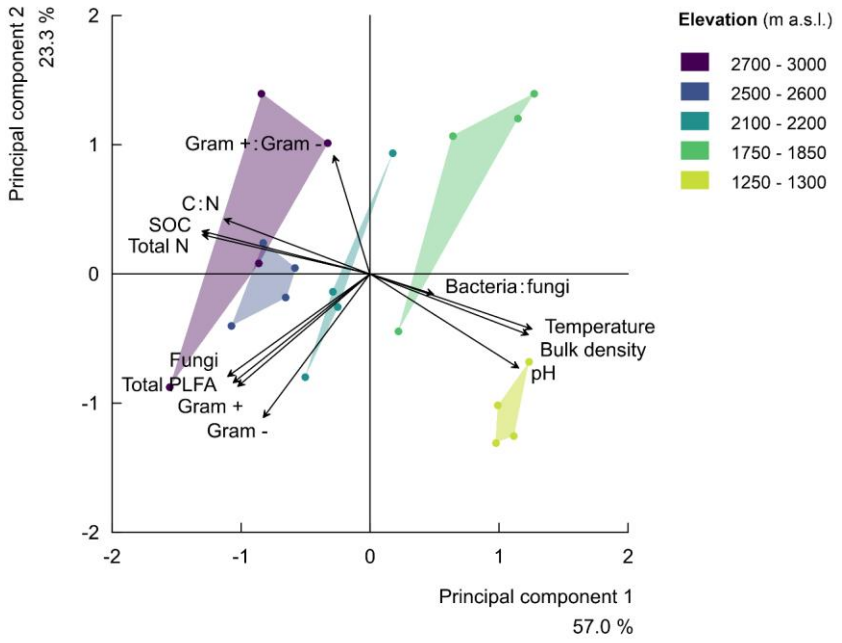

Figure 2. Principal component analysis (rescaled) of the relationships along the elevational gradient for soil physicochemical properties (i.e. the soil total nitrogen (total N), soil organic carbon (SOC), carbon-to-nitrogen ratio (C:N), soil pH (pH), soil temperature at 5 cm depth (temperature), bulk density) and the microbial community compositions (i.e. the bacteria to fungi ratio (bacteria:fungi) (total PLFA, in nmol g^{-1} soil), the ratio of gram-positive-to-gram-negative bacteria (gram+:gram-). The principal component 1 explained 57.0 % of the variability in studied parameters, while principal component 2 explained 23.3 % of the variability. The symbols of the individual plots on the biplot of the first two principal components are shown in different colours per elevation cluster.

3.2 Laboratory-based heterotrophic soil CO_2 respiration rate, AE and Q_{10}

The heterotrophic CO_2 respiration rates from laboratory incubations at corresponding mean *in situ* temperature only showed a significant difference when comparing elevation cluster at 2100-2200 m (CO_2 respiration rate of 0.71 ± 0.27 mg C h^{-1} kg^{-1}) with the elevation cluster at 2700-3000 m (CO_2 respiration rate of 0.55 ± 0.15 mg C h^{-1} kg^{-1}) (P = 0.025, SI Table 3). Furthermore, the heterotrophic CO_2 respiration rate at elevation cluster of 1750-1850 m was 0.51± 0.20 mg C h^{-1} kg^{-1} soil, which was statistically similar to the respiration rate of 0.55 ± 0.15 mg C h^{-1} kg^{-1} soil at the highest elevation cluster (2700-3000 m). Similarly, heterotrophic respiration rate of 0.67 ± 0.22 mg C h^{-1} kg^{-1} soil and of 0.64 ± 0.25 mg C h^{-1} kg^{-1} soil were recorded for the lowest elevation cluster (1250-1300 m) and the mid-elevation cluster at 2500-2600 m, respectively (SI Table 3). Consequently, heterotrophic CO_2 respiration rate from laboratory incubations showed a non-significant linear decrease at a rate of 0.004 ± 0.008 mg C h^{-1} kg^{-1} per 100 m of elevation increase (R^2_m = 0.007, P = 0.677, Table 2, Figure 3(a)).

In contrast, the specific heterotrophic CO_2 respiration rate (normalised per gram of SOC) revealed a significant linear trend along the elevational gradient. The highest CO_2 respiration rate of 17.2 ± 5.3 µg C h^{-1} g^{-1} SOC was detected at the lowest elevation cluster (1250-1300 m). This decreased to 10.8 ± 4.8 µg C h^{-1} g^{-1} SOC at 1750-1850 m and to 5.3 ± 2.1 µg C h^{-1} g^{-1} SOC at 2100-2200 m. Furthermore, lower values of 3.7 ± 1.9 µg C h^{-1} g^{-1} SOC and 2.4 ± 0.9 µg C h^{-1} g^{-1} SOC were observed at the highest two elevation clusters of 2500-2600 m and 2700-3000 m, respectively (SI Table 3). Generally, along the elevation gradient, the specific heterotrophic CO_2 respiration rate decreased linearly by 1.01 ± 0.12 µg C h^{-1} g^{-1} SOC per 100 m of elevation increase (R^2_m = 0.68, P = 0.003, Table 2, Figure 3(b)).

Further, following the decreasing trend in the specific heterotrophic CO_2 respiration rate along the elevational gradient, respired CO_2 indeed was more depleted in ^{13}C in warmer, lower elevations as compared to colder, higher elevations (Figure 3c). The ^{13}C depletion of the respired $\delta^{13}C$-CO_2 relative to $\delta^{13}C$-SOC was 3.2 ± 0.6 ‰ at 1250-1300 m, 2.8 ± 0.9 ‰ at 1750-1850 m, 1.7 ± 0.7 ‰ at 2100-2200 m, 1.0 ± 1.3 ‰ at 2500-2600 m and -0.3 ± 0.8 ‰ at 2700-3000 m (Figure 3(c), SI Table 3). Along the elevational gradient, the ^{13}C depletion of the respired CO_2 showed a significant linear decrease by 0.23 ± 0.04 ‰ per 100 m of elevation increase (R^2_m = 0.65, P = 0.011, Table 2, Figure 3(c)).

On the other hand, along the elevational gradient, AE ranged from 28.5 ± 5.6 kJ mol^{-1} in the premontane elevation cluster (1250-1300 m) to 70.3 ± 6.9 kJ mol^{-1} at 2500-2700 m and 69.9 ± 3.0 kJ mol^{-1} in the highest elevation cluster (2700-3000 m) (SI Table 3). Generally, along the elevational gradient, the AE showed a significant linear increase of 3.2 ± 0.7 kJ mol^{-1} per 100 m of elevation increase (R^2_m = 3.2, P < 001). Similarly, along the elevational gradient, Q_{10} values ranged from 1.50 ± 0.13 in the lowest elevation (1250-1300 m) to 2.68 ± 0.25 in the highest elevation (2700-3000 m), (SI Table 3). Generally, along the elevational gradient, the Q_{10} showed a linear increase of 0.09 ± 0.03 per 100 m of elevation increase (P = 0.012, Table 2, Figure 3(d)).

Deleted: a.s.l.
Deleted: a.s.l.
Deleted: SI,
Deleted: a.s.l.
Deleted: a.s.l.
Deleted: a.s.l.
Deleted: a.s.l.
Deleted: SI,
Deleted: a.s.l.
Deleted: a.s.l.
Deleted: a.s.l
Deleted: a.s.l
Deleted: a.s.l.
Deleted: SI,
Deleted: transect
Deleted: factor
Deleted: a.s.l.
Deleted: a.s.l.
Deleted: a.s.l.
Deleted: a.s.l.
Deleted: a.s.l.
Deleted: SI,
Deleted: factor
Deleted: a.s.l.
Deleted: a.s.l.
Deleted: a.s.l.
Deleted: SI,
Deleted: transect
Deleted: a.s.l.
Deleted: a.s.l
Deleted: SI,
Deleted: transect

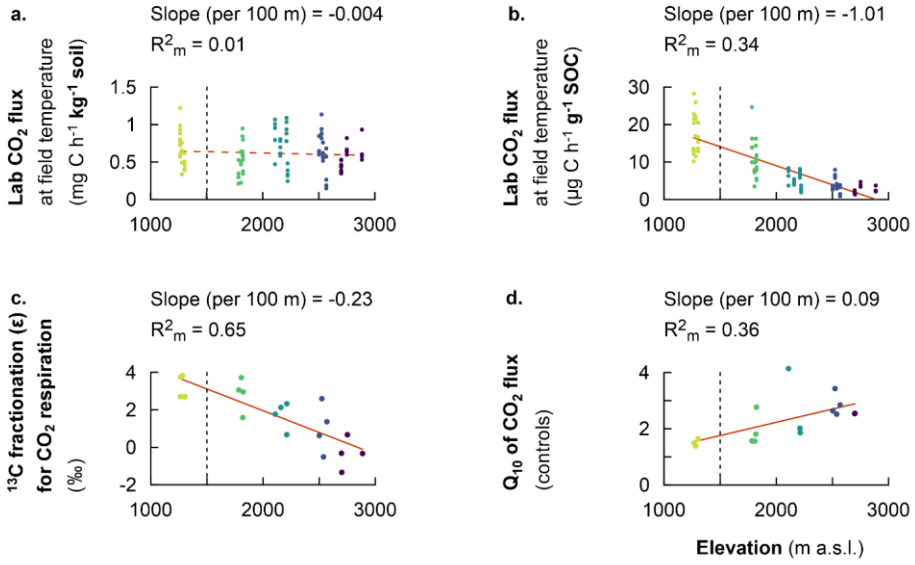

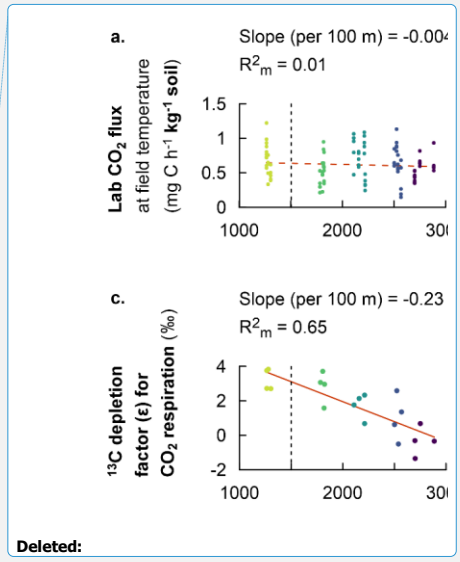

Deleted:

Figure 3. Fixed effect estimates of elevation (per 100 m elevation increase) on response parameters: laboratory-based heterotrophic CO_2 respiration rates at corresponding mean *in situ* temperature (a), and the specific heterotrophic CO_2 respiration rates at corresponding mean *in situ* temperature (b), the ^{13}C fractionation for heterotrophic CO_2 respiration (c), and the temperature sensitivity of heterotrophic CO_2 respiration rates (Q_{10}) (d). The slope of the linear mixed effect model estimates per 100 m of elevation increase is indicated (red solid line for a significant effect and red dashed line for no significant effect), as well as the marginal R^2 (R^2_m), representing the fraction of the response variable explained by elevation. Plots from montane forest clusters (from 1750-3000 m a.s.l.) were compared with a nearby premontane forest (separated by vertical dashed line) at an elevation of 1250-1300 m a.s.l.

Deleted: depletion factor

3.3 Effect of soil warming on CO_2 respiration, AE, Q_{10}, SOC and $\delta^{13}C$ values

After about 2 years of *in situ* soil warming, heterotrophic CO_2 respiration rates, AE and Q_{10} were assessed in a laboratory incubation experiment for control and warmed soil. Additionally, the SOC content and its $\delta^{13}C$ values for control and warmed soil were analysed. The results revealed that at each elevation cluster, there was no significant difference in the studied parameter between control and warmed soil (SI Table 3). However, along the entire elevational gradient, a consistent trend was observed, such that, both the non-specific and specific heterotrophic CO_2 respiration rates for controlled soil were relatively higher than those of warmed soil (Figure 4a and b respectively, SI Table 3). Similarly, along the elevational gradient, both the AE and Q_{10} coefficients for control were relatively higher than those of warmed soil (Figure 4c and d respectively). Additionally, after two years of *in situ* soil warming, the SOC contents of warmed soil were relatively lower than those of control along the elevational gradient (Figure 4(e)). Finally, the $\delta^{13}C$ values of the SOC showed that warmed soil became relatively more enriched in ^{13}C as compared to control soil (Figure 4(f)).

Deleted: SI,

Deleted: transect

Deleted: SI,

Deleted: transect

Deleted: composition

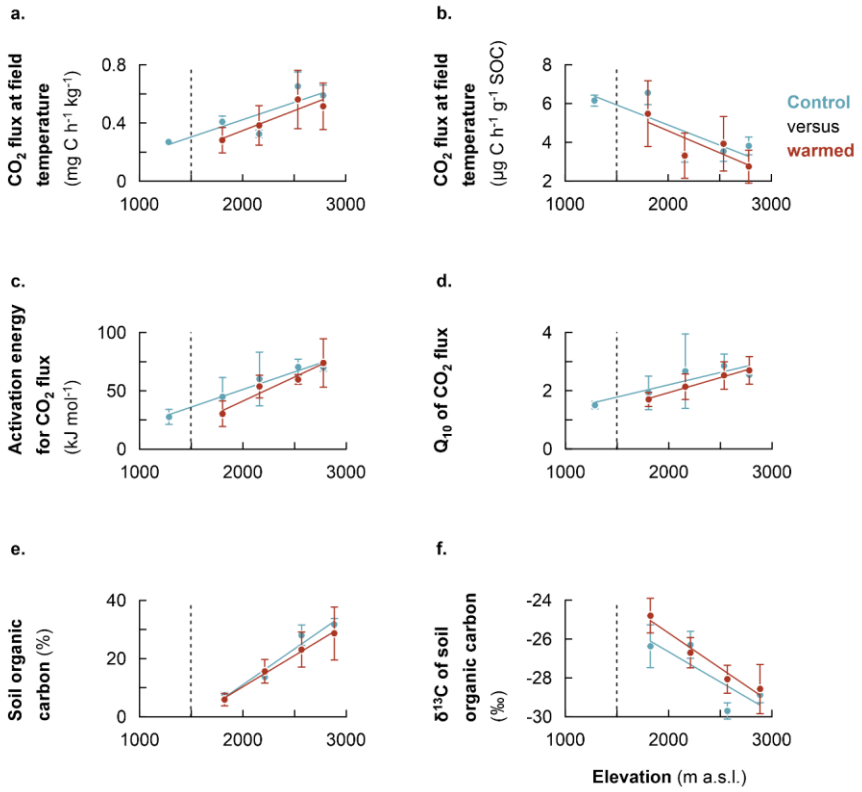

Figure 4. Comparison of warming response of soil organic carbon along the Rwenzori elevational gradient; heterotrophic CO_2 respiration rates of control and warmed soils (measured at the translocated *in situ* temperature) (a), idem for the specific CO_2 respiration rates (b), activation energy for control and warmed soil (c), sensitivity of CO_2 respiration rates to temperature (Q_{10}) for control and warmed (d), soil organic carbon content for control and warmed soil (e), and $\delta^{13}C$ values of soil organic carbon for control and warmed soil (f). Mean values were calculated from composite soil samples per elevation cluster (n = 4). The error bars indicate the standard deviation from the mean. For measurement of $\delta^{13}C$ values, the standard used was the international VPDB (Vee Pee Dee Belemnite).

Deleted: composition

3.4 *In situ* CO_2 respiration under current conditions at start and mid rainy season

The *in situ* total (heterotrophic and autotrophic) CO_2 respiration rates along the elevational gradient at the start of the rainy season were only significantly different when comparing the upper montane cluster (2700-3000 m) with the rest of the elevation clusters (1250-2200 m) (P = 0.027, SI Table 3). Total CO_2 respiration rate ranged from 95.1 ± 34.6 mg C m^{-2} h^{-1} in the lower montane elevation cluster at 2100-2200 m to 59.3 ± 16.7 mg C m^{-2} h^{-1} at 2700-3000 m. The total CO_2 respiration rate in the lower three elevations (1250-2200 m) were similar, ranging between 79.2 ± 17.3 mg C m^{-2} h^{-1} to 95.1 ± 34.6 mg C m^{-2} h^{-1} (SI Table 3). Generally, along the elevational gradient, there was no significant linear trend in the total CO_2 respiration rate, though this tended to decrease at a rate of 1.04 ± 1.49 mg C m^{-2} h^{-1} per 100 m of elevation increase at the start of rainy season (R^2_m =0.04, P =0.558, Table 2, SI Figure 3).

On the other hand, in the mid rainy season, there was a much stronger variability in the *in situ* total CO_2 respiration rates among the elevation clusters (P < 0.001, SI Table 3). The total CO_2 respiration rate was highest (i.e. 113.2 ± 35.7 mg C m^{-2} h^{-1}) in the premontane elevation cluster at 1250-1300 m. A statistically similar respiration rate of 112.8 ± 20.3 mg C m^{-2} h^{-1} was found in the montane foothill at 1750-1850 m. There was a significantly lower total CO_2 respiration rate (i.e. 89.0 ± 22.3 mg C m^{-2} h^{-1}) at 2100-2200 m, which further decreased to 67.7 ± 9.6 mg C m^{-2} h^{-1} at 2700-3000 m (SI Table 3). Overall, along the elevational gradient, there was also no significant linear trend in the total CO_2 respiration rate which tended to decrease at a rate of 3.25 ± 0.89 mg C m^{-2} h^{-1} per 100 m of elevation increase (R^2_m = 0.33, P = 0.067, Table 2, SI Figure 3).

Comparison of seasonal *in situ* total CO_2 respiration rates generally revealed that higher soil moisture contents were associated with higher CO_2 respiration rates. Specifically, at 1250-1300 m, total CO_2 respiration rate at the start of the rainy season (80.1 ± 15.8 mg C m^{-2} h^{-1}) increased significantly to 113.2 ± 9.6 mg C m^{-2} h^{-1} in the mid rainy season (P < 0.001, SI Table 3). Similarly, the total CO_2 respiration rate at 1750-1850 m increased significantly from 79.2 ± 17.3 mg C m^{-2} h^{-1} at the start of the rainy season to 112.8 ± 20.3 mg C m^{-2} h^{-1} in the mid rainy season (P < 0.001). There was no seasonal variation in the total CO_2 respiration rate at 2100-2200 m, where the total CO_2 respiration rate was between 95.1 ± 34.6 mg C m^{-2} h^{-1} and 89.0 ± 22.3 mg C m^{-2} h^{-1} in the start and the mid rainy season, respectively. At 2700-3000 m, the total CO_2 respiration rate increased significantly from 59.3 ± 16.7 mg C m^{-2} h^{-1} in the start of rainy season to 67.7 ± 9.6 mg C m^{-2} h^{-1} in the mid rainy season (P = 0.035, SI Table 3).

Deleted: a.s.l.
Deleted: a.s.l.
Deleted: SI,
Deleted: a.s.l.
Deleted: a.s.l.
Deleted: a.s.l.
Deleted: SI,
Deleted: SI,
Deleted: SI,
Deleted: a.s.l..
Deleted: a.s.l.
Deleted: a.s.l.
Deleted: a.s.l.
Deleted: SI,
Deleted: SI,
Deleted: a.s.l.
Deleted: SI,
Deleted: a.s.l.
Deleted: a.s.l.
Deleted: SI,

Table 2. Fixed effect estimates of elevation (per 100 m elevation increase) on selected soil parameters The associated standard error (SE), *P*-value, marginal coefficient of determination (R^2_m) and conditional coefficient of determination (R^2_c) are indicated.

Parameters	Effect estimate	SE	*P*-value	R^2_m	R^2_c
Laboratory-based CO_2 respiration ($\mu g\ CO_2\text{-}C\ h^{-1}\ kg^{-1}$ soil)	-0.00	0.01	0.680	0.01	0.12
Laboratory-based specific CO_2 respiration (mg CO_2-C h^{-1} g^{-1} SOC)	**-1.01**	**0.12**	**0.003***	**0.68**	**0.72**
^{13}C fractionation for respired CO_2 (ε) (‰)	**-0.23**	**0.04**	**0.011***	**0.65**	**0.66**
Q_{10} control	**0.09**	**0.03**	**0.012***	**0.36**	**0.36**
Q_{10} warmed	**0.09**	**0.03**	**0.013***	**0.37**	**0.37**
SOC - control (%)	**2.63**	**0.33**	**0.008****	**0.91**	**0.96**
SOC - warmed (%)	2.33	0.37	> 0.001***	0.73	0.73
$\delta^{13}C$ -SOC- control	-0.31	0.15	0.132	0.44	0.82
$\delta^{13}C$-SOC - warmed	**-0.40**	**0.06**	**> 0.001*** **	**0.75**	**0.75**
STN - control (%)	**0.17**	**0.03**	**0.024***	**0.82**	**0.92**
STN - warmed (%)	**0.14**	**0.03**	**> 0.001*** **	**0.67**	**0.67**
$\delta^{15}N$ - control (‰)	**-0.55**	**0.13**	**0.030***	**0.75**	**0.95**
$\delta^{15}N$ - warmed (‰)	**-0.62**	**0.07**	**> 0.001*** **	**0.85**	**0.85**
Specific CO_2 respiration - control ($\mu g\ C\ g^{-1}$ SOC)	-0.09	0.15	0.573	0.05	0.92
Specific CO_2 respiration - warmed $\mu g\ C\ g^{-1}$ SOC	-0.20	0.11	0.229	0.23	0.36
CO_2 respiration at start of rainy season ($mg\ CO_2\text{-}C\ h^{-1}\ m^{-2}$)	-1.04	1.49	0.558	0.04	0.35
CO_2 respiration in mid rainy season ($mg\ CO_2\text{-}C\ h^{-1}\ m^{-2}$)	-3.25	0.89	0.067	0.33	0.40

A statistically significant elevational linear trend is bolded, and *P*-value marked with asterisk symbol "*", R^2_m is the proportion of the variance in the response variable explained by the fixed effect (elevation), R^2_c is the proportion of the variance in the response variable explained by the fixed effect plus random location effects.

Deleted: heterotrophic CO_2 respiration rates under laboratory incubations at corresponding mean *in situ* temperature, laboratory-based heterotrophic specific CO_2 respiration (normalised per unit soil organic carbon (SOC)), ^{13}C depletion factor for CO_2 respiration (ε), and temperature sensitivity of CO_2 respiration rate (Q_{10}) for control and warmed soil, and *in situ* total CO_2 respiration rates at the start and in the mid rainy season along the elevational transect.

Formatted Table

Deleted: depletion factor

Deleted: respiration

Formatted: Font: Bold

Formatted: Font: Bold

4 Discussion

4.1 Elevational trend in CO_2 respiration, ^{13}C fractionation of the respired CO_2 and Q_{10}

The specific heterotrophic CO_2 respiration decreased along elevation in part, due to negative effect of low temperature on microbial activity (Zimmermann et al., 2009). In support of the temperature effect on CO_2 respiration (Figure 3(b)), the apparent ^{13}C fractionation for SOC transformation was also temperature dependent. The emitted CO_2 at the warm, lower elevations showed a higher apparent fractionation (and subsequently became relatively more depleted in ^{13}C) than at the cold, higher elevations (Figure 3(c)). This observation may result from either a shift in the use of C substrates along the temperature gradient or ^{13}C discrimination during SOC decomposition by micro-organisms (Andrews et al., 2000; Ehleringer et al., 2000; Natelhoffer and Fry, 1988). Indeed, the N stable isotope composition also indicated a decrease in $\delta^{15}N$ values with elevation (Table 1). This indicates a more closed N cycling and reduced N transformation with increasing elevation, characterised by low N losses (Amundson et al., 2003; Boeckx et al., 2005). Similarly, the observed higher apparent ^{13}C fractionation indicates differences in the rate of soil organic matter transformation across different elevations. Altogether, these results imply that at higher elevations, even though SOC contents were high, microbial decomposition was limited by low temperatures (Zimmermann et al., 2009). In addition, low CO_2 respiration at high elevations is likely explained by the inhibitory effect of the low soil pH on microbial respiration (Figure 3(c), SI Table 1) (Rousk et al., 2009) impairing microbial activity (Walse et al., 1998). Further, low pH is also known to facilitate the stabilisation of organic matter through complexation reactions with iron and aluminum ions, which become soluble at a low pH (Lützow et al., 2006).

Additionally, the observed linear increases in Q_{10} and AE with elevation (Table 2, Figure 3(d)), indicate an increasing trend in soil organic matter recalcitrance resulting in lower specific CO_2 respiration at high elevations (Davidson and Janssens, 2006). This is corroborated by the decreasing apparent ^{13}C fractionation (Table 2, Figure 3(c)), as well as lower specific heterotrophic CO_2 respiration in higher elevations at a uniform temperature and 60 % WFPS (r= -0.53, P = 0.02, SI Table 2, SI Figure 5). The linearly increasing elevational trend in AE and Q_{10} is consistent with the intrinsic principles of microbial respiration kinetics associated with the Arrhenius equation (Craine et al., 2010; Davidson and Janssens, 2006; Schipper et al., 2014). Accordingly, the sensitivity of microbial decomposition to an increment in temperature should increase with increasing AE and recalcitrance of the substrate (Craine et al., 2010; Luo et al., 2001; Davidson and Janssens, 2006). As such, more complex (i.e. recalcitrant) C compounds, for which the microbial decomposition requires more AE, render a lower specific heterotrophic CO_2 respiration (SI Figure 5) and a higher Q_{10} (i.e. their decomposition is enhanced to a higher extent at a certain increase in temperature) than more simple (i.e. labile) C substrates (Craine et al., 2010; Davidson and Janssens, 2006; Nottingham et al., 2019).

Deleted: Q_{10} and
Deleted: depletion factor
Formatted: Subscript
Deleted: factor for
Deleted: respiration
Deleted: , such
Deleted: that the respired
Deleted: ,
Deleted: z
Deleted: also indicates that the higher the specific heterotrophic respiration rates, the higher the discrimination against the heavier ^{13}C isotope (Andrews et al., 2000; Natelhoffer and Fry, 1988)
Deleted: SOC
Deleted: is
Deleted: SI,
Deleted: the
Deleted: s
Deleted: SI,
Deleted: SI,
Deleted: facilitates
Deleted: SI,

4.2 Effect of *in situ* warming

Generally, after two years of *in situ* warming, $\delta^{13}C$ values of SOC revealed a relative enrichment in ^{13}C in warmed soil as compared to the control (Figure 4(f)). This is consistent with the observation of ^{13}C depleted C losses during microbial CO_2 respiration (Figure 3(c). The relative enrichment in ^{13}C in warmed soil as compared to the control is likely due to enhanced mineralisation rates in the warmed soil. Higher mineralisation causes a change in ^{13}C fractionation due to change in C substrate (following depletion of most labile C) and/or microbial discrimination against ^{13}C during C transformation processes (Andrews et al., 2000; Ehleringer et al., 2000; Natelhoffer and Fry, 1988). Altogether, these results (increase in organic matter transformation and likely change of C substrate following depletion of most labile C) imply that warming indeed increased mineralisation of SOC in warmed relative to control soil, owing to the increase in microbial activity at higher temperatures in correspondence with the Arrhenius equation (Craine et al., 2010; Mohan, 2019; Nottingham et al., 2020). Indeed, along the elevational gradient, SOC was relatively lower in warmed as compared to control (Figure 4(e)). Subsequently, the CO_2 respiration for warmed soils were relatively lower than in the controls due to the apparent depletion of respiration substrate during the two years of warming. The evidence of accelerated mineralisation of SOC upon warming supports the results of several soil warming studies that reported an increment in CO_2 respiration upon warming (Eliasson et al., 2005; Luo et al., 2001; Melillo et al., 2002; Rustad et al., 2001). The increased decomposition following a temperature increase has the ability to inherently change the content and quality of the SOC, if organic inputs cannot replenish SOC loss at the same rate (Craine et al., 2010; Davidson and Janssens, 2006; Luo et al., 2001). Nonetheless, the lack of significant difference in CO_2 respiration rates for warmed and control soil at each elevation cluster after two years of warming may also indicate the fact that labile SOC fractions were not depleted after two years at a higher temperature (Crowther et al., 2016; Davidson and Janssens, 2006; Melillo et al., 2017).

On the other hand, along the elevational gradient, the AE and Q_{10} values of warmed soils were relatively lower than in the control soils (Figure 4(c) and (d) respectively). This trend is expected as the Arrhenius equation predicts that the Q_{10} of a certain reaction intrinsically decreases with increasing temperature (Craine et al., 2010; Davidson and Janssens, 2006). As such, SOC substrates would become overall less recalcitrant after two years at an elevated temperature. Indeed, while warming increases the mineralisation rate of the most labile C, it also stimulates the decomposition of recalcitrant C fractions to a relative higher degree than labile fractions because of the higher Q_{10} of the former (Craine et al., 2010; Davidson and Janssens, 2006). Subsequently, the AE and Q_{10} of warmed soils were relatively lower than those of the controls (Davidson and Janssens, 2006; Mohan, 2019; Nottingham et al., 2020). Both the decrease in SOC contents and the relatively enhanced activation of recalcitrant organic matter upon warming undermine the climate mitigation function of the soil (Davidson and Janssens, 2006; Nottingham et al., 2020; Walker et al., 2018).

Deleted: isotope
Formatted: Superscript
Formatted: Subscript
Deleted: is
Deleted: stronger
Deleted: (Amundson et al., 2003), due to
Deleted: (Andrews et al., 2000; Natelhoffer and Fry, 1988)
Deleted: T
Deleted: transect
Deleted: transect

We note that the lack of significant difference in CO_2 flux and associated selected parameters at each elevation cluster may be due to the too short duration of the warming experiment. Additionally, high spatial variability in soil properties and environmental conditions (e.g. variation in slope and aspect), often preclude powerful statistical tests for small treatment effects (Davidson and Janssens, 2006), as is usually the case in warming experiments. Further, warming may result in a trade-off effect on SOC respiration. For instance, increased mineralisation rates upon warming are expected to reduce SOC (Nottingham et al., 2019). Similarly, higher litter input and turn-over at lower elevations (Okello et al., 2022), is expected to increase SOC. As such, the trade-off effect of these processes likely dampened the net effect of (short-term) warming on SOC transformation processes.

4.3 Present-day CO_2 respiration along the Rwenzori elevational gradient

Along the Rwenzori Mountains elevational gradient, we observed that the *in situ* total CO_2 respiration rates were significantly lower at the highest elevation cluster of the montane forest in both the start and the mid rainy season as compared to premontane forest. On the other hand, by isolating the effect of moisture in a laboratory incubation (at uniform 60 % WFPS and corresponding *in situ* measured temperatures per elevation cluster), we found similar heterotrophic CO_2 respiration along the elevational gradient (SI Table 3, Figure 3(a)), and ultimately, we confirmed a significant linearly decreasing trend for the specific heterotrophic CO_2 respiration (Figure 3(b)). This indicates that, under *in situ* condition, low temperatures and low soil moisture contents limited microbial CO_2 respiration at high elevations. Indeed low temperatures at high elevations can have a negative effect on decomposer activities (Finzi et al., 2006; Luo et al., 2006). Meanwhile, an adequate soil moisture content can boost microbial respiration by facilitating both the diffusion of soluble substrates and the transport of oxygen (Liu et al., 2006). Generally, the optimal soil moisture content for microbial respiration is reported to be approximately 60 % WFPS (Aon et al., 2001; Doetterl et al., 2015). Subsequently, in the mid rainy season (when the soil WFPS increased) (SI Table 3), in correspondence, we detected an increase in the total *in situ* CO_2 respiration rate in all elevation clusters, but at higher elevations between 2100-3000 m, the increase in CO_2 respiration rates were not significant owing to only a small increase in WFPS in the mid rainy season (SI Table 3).

The microbial community structure indicated that though the variation of the microbial community (in terms of bacteria and fungi), as a function of elevation is rather limited (SI Figure 4), there is some shift. In particular, higher elevations are relatively more dominated by gram-positive bacteria (Figure 4, SI Table 2) and by fungi relative to bacteria (SI Figure 4), which is also further indictor for higher organic matter recalcitrance (Fanin et al., 2019; Lipson et al., 2002). Based on the principal component analysis and linear mixed effect model analysis of microbial structure (Figure 4, SI Figure 4), the ratio of total bacteria to fungi slightly decreased with increasing elevation. It is also known that fungi are often relatively more dominant in soils characterised by more complex organic materials (Lipson et al., 2002), as fungi are more specialised in the breakdown of recalcitrant organic matter (Boer et al., 2005; Coleman et al., 2017). Altogether, we showed that microbial CO_2 respiration

Deleted: ,

Deleted: transect

Deleted: transect

Deleted: transect

Deleted: SI,

Deleted: SI,

Deleted: a.s.l.

Deleted: SI,

Deleted: SI,

Deleted: SI,

Deleted: SI,

Deleted: SI,

Deleted: ,

Deleted: where i

along the elevational gradient was limited by an increasing C recalcitrance, decreasing soil temperature, moisture content and pH.

5 Conclusion

Our results indicated that global warming can lead to enhanced losses of SOC in montane forests due to their increasing temperature sensitivity and SOC content with elevation. Therefore, the high concentrations of SOC at higher elevations of montane forests are particularly at stake, since the climate warming exactly undermines the mitigating effect of low microbial decomposition under: (i) low temperature; and (ii) high organic matter recalcitrance (due its higher temperature sensitivity). Further, we showed that along the elevational gradient, *in situ* warming indeed led to increased SOC mineralisation and the associated apparent isotopic fractionation resulted in a relative enrichment in ^{13}C in warmed soils as compared to the controls. Ultimately, along the elevational gradient, after two years of warming, the SOC in the warmed soils were relatively lower than in the controls, indicating a depleting trend in SOC owing to the increment in mineralisation during the two years at higher temperature.

Deleted: transect

Deleted: carbon

Deleted: ;

Deleted: of

Deleted: isotope

Deleted: This is due to stronger discrimination against the ^{13}C isotope owing to faster SOC transformation processes.

Acknowledgement

This work was funded by VLIR-UOS and Mountains of the Moon University under the partnership program of Inter-University Cooperation (IUC), grant number UG2019IUC027A103. The authors thank Uganda Wildlife Authority for granting permission to conduct this study in two protected National Parks under permit number UWA/COD/96/05. We also thank staff of the Uganda Wildlife Authority at Rwenzori Mountains and Kibale Forest National Parks for their support. Further, we are grateful to the Research Assistant, Mr. Martin Tuisenge for his tireless efforts and endurance during the demanding field campaigns in the tremendously physically challenging Rwenzori Mountains.

Disclosure statement

The authors declare that they have no conflict of interest

References

Andrews, J. A., Matamala, R., Westover, K. M., and Schlesinger, W. H.: Temperature effects on the diversity of soil heterotrophs and the δ13C of soil-respired CO2, Soil Biology and Biochemistry, 32, 699-706, https://doi.org/10.1016/S0038-0717(99)00206-0, 2000.

Aon, M., Sarena, D., Burgos, J., and Cortassa, S.: Interaction between gas exchange rates, physical and microbiological properties in soils recently subjected to agriculture, Soil and Tillage Research, 60, 163-171, https://doi.org/10.1016/S0167-1987(01)00191-X, 2001.

Beer, C., Reichstein, M., Tomelleri, E., Ciais, P., Jung, M., Carvalhais, N., Rödenbeck, C., Arain, M. A., Baldocchi, D., and Bonan, G. B.: Terrestrial gross carbon dioxide uptake: global distribution and covariation with climate, Science, 329, 834-838, https://doi.org/10.1126/science.1184984, 2010.

Bligh, E. G. and Dyer, W. J.: A rapid method of total lipid extraction and purification, Canadian journal of biochemistry and physiology, 37, 911-917, https://doi.org/10.1139/o59-099, 1959.

Boer, W. d., Folman, L. B., Summerbell, R. C., and Boddy, L.: Living in a fungal world: impact of fungi on soil bacterial niche development, FEMS microbiology reviews, 29, 795-811, https://doi.org/10.1016/j.femsre.2004.11.005, 2005.

Bradford, M. A., Davies, C. A., Frey, S. D., Maddox, T. R., Melillo, J. M., Mohan, J. E., Reynolds, J. F., Treseder, K. K., and Wallenstein, M. D.: Thermal adaptation of soil microbial respiration to elevated temperature, Ecology letters, 11, 1316-1327, https://doi.org/10.1111/j.1461-0248.2008.01251.x, 2008.

Campbell, D. J. and Henshall, J. K.: Bulk density, in: Soil and Environmental Analysis, CRC Press, 327-360, 2000.

Carey, J. C., Tang, J., Templer, P. H., Kroeger, K. D., Crowther, T. W., Burton, A. J., Dukes, J. S., Emmett, B., Frey, S. D., and Heskel, M. A.: Temperature response of soil respiration largely unaltered with experimental warming, Proceedings of the National Academy of Sciences, 113, 13797-13802, https://doi.org/10.1073/pnas.1605365113, 2016.

Chung, H., Zak, D. R., Reich, P. B., and Ellsworth, D. S.: Plant species richness, elevated CO2, and atmospheric nitrogen deposition alter soil microbial community composition and function, Global Change Biology, 13, 980-989, https://doi.org/10.1111/j.1365-2486.2007.01313.x, 2007.

Coleman, D. C., Callaham, M. A., and Crossley Jr, D.: Fundamentals of soil ecology, Academic press2017.

Collier, S. M., Ruark, M. D., Oates, L. G., Jokela, W. E., and Dell, C. J.: Measurement of greenhouse gas flux from agricultural soils using static chambers, Journal of visualized experiments: JoVE, https://doi.org/10.3791/52110, 2014.

Craine, J. M., Fierer, N., and McLauchlan, K. K.: Widespread coupling between the rate and temperature sensitivity of organic matter decay, Nature Geoscience, 3, 854-857, https://doi.org/10.1038/ngeo1009, 2010.

Crowther, T. W., Todd-Brown, K. E., Rowe, C. W., Wieder, W. R., Carey, J. C., Machmuller, M. B., Snoek, B., Fang, S., Zhou, G., and Allison, S. D.: Quantifying global soil carbon losses in response to warming, Nature, 540, 104-108, https://doi.org/10.1038/nature20150, 2016.

Cuni Sanchez, A., Sullivan, M., Platts, P. J., Lewis, S. L., Marchant, R., Imani, G., Hubau, W., Abiem, I., Adhikari, H., and Albrecht, T.: High aboveground carbon stock of African tropical montane forests, Nature, https://doi.org/10.1038/s41586-021-03728-4, 2021.

Dalal, R., Allen, D., Livesley, S., and Richards, G.: Magnitude and biophysical regulators of methane emission and consumption in the Australian agricultural, forest, and submerged landscapes: a review, Plant and Soil, 309, 43-76, https://doi.org/10.1007/s11104-007-9446-7, 2008.

Davidson, E. A. and Janssens, I. A.: Temperature sensitivity of soil carbon decomposition and feedbacks to climate change, Nature, 440, 165-173, https://doi.org/10.1038/nature04514, 2006.

Denef, K., Bubenheim, H., Lenhart, K., Vermeulen, J., Van Cleemput, O., Boeckx, P., and Müller, C.: Community shifts and carbon translocation within metabolically-active rhizosphere microorganisms in grasslands under elevated CO 2, Biogeosciences, 4, 769-779, https://doi.org/10.5194/bg-4-769-2007, 2007.

Doetterl, S., Stevens, A., Six, J., Merckx, R., Van Oost, K., Pinto, M. C., Casanova-Katny, A., Muñoz, C., Boudin, M., and Venegas, E. Z.: Soil carbon storage controlled by interactions between geochemistry and climate, Nature Geoscience, 8, 780-783, https://doi.org/10.1038/ngeo2516, 2015.

Drijber, R. A., Doran, J. W., Parkhurst, A. M., and Lyon, D.: Changes in soil microbial community structure with tillage under long-term wheat-fallow management, Soil Biology and Biochemistry, 32, 1419-1430, https://doi.org/10.1016/S0038-0717(00)00060-2, 2000.

Ehleringer, J. R., Buchmann, N., and Flanagan, L. B.: Carbon isotope ratios in belowground carbon cycle processes, Ecological Applications, 10, 412-422, https://doi.org/10.1890/1051-0761(2000)010[0412:CIRIBC]2.0.CO;2, 2000.

Eliasson, P. E., McMurtrie, R. E., Pepper, D. A., Strömgren, M., Linder, S., and Ågren, G. I.: The response of heterotrophic CO2 flux to soil warming, Global Change Biology, 11, 167-181, https://doi.org/10.1111/j.1365-2486.2004.00878.x, 2005.

Erb, K.-H., Kastner, T., Plutzar, C., Bais, A. L. S., Carvalhais, N., Fetzel, T., Gingrich, S., Haberl, H., Lauk, C., and Niedertscheider, M.: Unexpectedly large impact of forest management and grazing on global vegetation biomass, Nature, 553, 73-76, https://doi.org/10.1038/nature25138, 2018.

Fanin, N., Kardol, P., Farrell, M., Nilsson, M.-C., Gundale, M. J., and Wardle, D. A.: The ratio of Gram-positive to Gram-negative bacterial PLFA markers as an indicator of carbon availability in organic soils, Soil Biology and Biochemistry, 128, 111-114, https://doi.org/10.1016/j.soilbio.2018.10.010, 2019.

Findlay, R. H., King, G. M., and Watling, L.: Efficacy of phospholipid analysis in determining microbial biomass in sediments, Applied and Environmental Microbiology, 55, 2888-2893, https://doi.org/10.1128/aem.55.11.2888-2893.1989, 1989.

Finzi, A. C., Moore, D. J., DeLucia, E. H., Lichter, J., Hofmockel, K. S., Jackson, R. B., Kim, H.-S., Matamala, R., McCarthy, H. R., and Oren, R.: Progressive nitrogen limitation of ecosystem processes under elevated CO2 in a warm-temperate forest, Ecology, 87, 15-25, https://doi.org/10.1890/04-1748, 2006.

Friedlingstein, P., O'sullivan, M., Jones, M. W., Andrew, R. M., Hauck, J., Olsen, A., Peters, G. P., Peters, W., Pongratz, J., and Sitch, S.: Global carbon budget 2020, Earth System Science Data, 12, 3269-3340, https://doi.org/10.5194/essd-12-3269-2020, 2020.

Frostegård, A. and Bååth, E.: The use of phospholipid fatty acid analysis to estimate bacterial and fungal biomass in soil, Biology and Fertility of soils, 22, 59-65, https://doi.org/10.1007/BF00384433, 1996.
Fussmann, K. E., Schwarzmüller, F., Brose, U., Jousset, A., and Rall, B. C.: Ecological stability in response to warming, Nature Climate Change, 4, 206-210, https://doi.org/10.1038/nclimate2134, 2014.
Gütlein, A., Gerschlauer, F., Kikoti, I., and Kiese, R.: Impacts of climate and land use on N2O and CH 4 fluxes from tropical ecosystems in the Mt. Kilimanjaro region, Tanzania, Global change biology, 24, 1239-1255, https://doi.org/10.1111/gcb.13944, 2018.
Huygens, D., Roobroeck, D., Cosyn, L., Salazar, F., Godoy, R., and Boeckx, P.: Microbial nitrogen dynamics in south central Chilean agricultural and forest ecosystems located on an Andisol, Nutrient Cycling in Agroecosystems, 89, 175-187, https://doi.org/10.1007/s10705-010-9386-0, 2011.
IPCC: Global warming of 1.5° C: an IPCC special report on the impacts of global warming of 1.5° C above pre-industrial levels and related global greenhouse gas emission pathways, in the context of strengthening the global response to the threat of climate change, sustainable development, and efforts to eradicate poverty, Intergovernmental Panel on Climate Change2018.
IPCC: Summary for Policymakers. In: Climate Change 2021: The Physical Science Basis. Contribution of Working Group I to the Sixth Assessment Report of the Intergovernmental Panel on Climate Change, 2021.
Jacobs, L., Dewitte, O., Poesen, J., Delvaux, D., Thiery, W., and Kervyn, M.: The Rwenzori Mountains, a landslide-prone region?, Landslides, 13, 519-536, https://doi.org/10.1007/s10346-015-0582-5, 2016.
Karhu, K., Auffret, M. D., Dungait, J. A., Hopkins, D. W., Prosser, J. I., Singh, B. K., Subke, J.-A., Wookey, P. A., Ågren, G. I., and Sebastia, M.-T.: Temperature sensitivity of soil respiration rates enhanced by microbial community response, Nature, 513, 81-84, https://doi.org/10.1038/nature13604, 2014.
Keane, J. B. and Ineson, P.: Differences in the diurnal pattern of soil respiration under adjacent Miscanthus× giganteus and barley crops reveal potential flaws in accepted sampling strategies, Biogeosciences, 14, 1181-1187, https://doi.org/10.5194/bg-14-1181-2017, 2017.
Kim, D.-G., Thomas, A. D., Pelster, D., Rosenstock, T. S., and Sanz-Cobena, A.: Greenhouse gas emissions from natural ecosystems and agricultural lands in sub-Saharan Africa: synthesis of available data and suggestions for further research, Biogeosciences, 13, 4789-4809, https://doi.org/10.5194/bg-13-4789-2016, 2016.
Kroppenstedt, R.: Fatty acid and menaquinone analysis of actinomycetes and related organisms, Chemical methods in bacterial systematics, 173-199, 1985.
Kutzbach, L., Schneider, J., Sachs, T., Giebels, M., Nykänen, H., Shurpali, N., Martikainen, P., Alm, J., and Wilmking, M.: CO 2 flux determination by closed-chamber methods can be seriously biased by inappropriate application of linear regression, Biogeosciences, 4, 1005-1025, https://doi.org/10.5194/bg-4-1005-2007, 2007.
Lewis, S. L., Edwards, D. P., and Galbraith, D.: Increasing human dominance of tropical forests, Science, 349, 827-832, https://doi.org/10.1126/science.aaa9932, 2015.
Lipson, D. A., Schadt, C., and Schmidt, S. K.: Changes in soil microbial community structure and function in an alpine dry meadow following spring snow melt, Microbial ecology, 43, 307-314, https://doi.org/10.1007/s00248-001-1057-x, 2002.

Liu, H. S., Li, L. H., Han, X. G., Huang, J. H., Sun, J. X., and Wang, H. Y.: Respiratory substrate availability plays a crucial role in the response of soil respiration to environmental factors, Applied Soil Ecology, 32, 284-292, https://doi.org/10.1016/j.apsoil.2005.08.001, 2006.
Luo, Y., Field, C. B., and Jackson, R. B.: Does Nitrogen Constrain Carbon Cycling, or Does Carbon Input Stimulate Nitrogen Cycling? 1, Ecology, 87, 3-4, 2006.
Luo, Y., Wan, S., Hui, D., and Wallace, L. L.: Acclimatization of soil respiration to warming in a tall grass prairie, Nature, 413, 622-625, https://doi.org/10.1038/35098065, 2001.
Lützow, M. v., Kögel-Knabner, I., Ekschmitt, K., Matzner, E., Guggenberger, G., Marschner, B., and Flessa, H.: Stabilization of organic matter in temperate soils: mechanisms and their relevance under different soil conditions–a review, European journal of soil science, 57, 426-445, https://doi.org/10.1111/j.1365-2389.2006.00809.x, 2006.
Mahmood, R., Pielke Sr, R. A., Hubbard, K. G., Niyogi, D., Dirmeyer, P. A., McAlpine, C., Carleton, A. M., Hale, R., Gameda, S., and Beltrán-Przekurat, A.: Land cover changes and their biogeophysical effects on climate, International journal of climatology, 34, 929-953, https://doi.org/10.1002/joc.3736, 2014.
Malhi, Y.: The productivity, metabolism and carbon cycle of tropical forest vegetation, Journal of Ecology, 100, 65-75, https://doi.org/10.1111/j.1365-2745.2011.01916.x, 2012.
Melillo, J., Steudler, P., Aber, J., Newkirk, K., Lux, H., Bowles, F., Catricala, C., Magill, A., Ahrens, T., and Morrisseau, S.: Soil warming and carbon-cycle feedbacks to the climate system, Science, 298, 2173-2176, https://doi.org/10.1126/science.1074153, 2002.
Melillo, J. M., Frey, S. D., DeAngelis, K. M., Werner, W. J., Bernard, M. J., Bowles, F. P., Pold, G., Knorr, M. A., and Grandy, A. S.: Long-term pattern and magnitude of soil carbon feedback to the climate system in a warming world, Science, 358, 101-105, https://doi.org/10.1126/science.aan2874, 2017.
Mohan, J. E.: Ecosystem Consequences of Soil Warming: Microbes, Vegetation, Fauna and Soil Biogeochemistry, Academic Press2019.
Nakagawa, S. and Schielzeth, H.: A general and simple method for obtaining R2 from generalized linear mixed-effects models, Methods in ecology and evolution, 4, 133-142, https://doi.org/10.1111/j.2041-210x.2012.00261.x, 2013.
Natelhoffer, K. and Fry, B.: Controls on natural nitrogen-15 and carbon-13 abundances in forest soil organic matter, Soil Science Society of America Journal, 52, 1633-1640, https://doi.org/10.2136/sssaj1988.03615995005200060024x, 1988.
Nazaries, L., Tottey, W., Robinson, L., Khachane, A., Al-Soud, W. A., Sørensen, S., and Singh, B. K.: Shifts in the microbial community structure explain the response of soil respiration to land-use change but not to climate warming, Soil Biology and Biochemistry, 89, 123-134, https://doi.org/10.1016/j.soilbio.2015.06.027, 2015.
Nottingham, A. T., Meir, P., Velasquez, E., and Turner, B. L.: Soil carbon loss by experimental warming in a tropical forest, Nature, 584, 234-237, https://doi.org/10.1038/s41586-020-2566-4, 2020.
Nottingham, A. T., Whitaker, J., Ostle, N. J., Bardgett, R. D., McNamara, N. P., Fierer, N., Salinas, N., Ccahuana, A. J., Turner, B. L., and Meir, P.: Microbial responses to warming enhance soil carbon loss following translocation across a tropical forest elevation gradient, Ecology letters, 22, 1889-1899, 2019.
Oertel, C., Matschullat, J., Zurba, K., Zimmermann, F., and Erasmi, S.: Greenhouse gas emissions from soils—A review, Geochemistry, 76, 327-352, https://doi.org/10.1016/j.chemer.2016.04.002, 2016.

Okello, J., Bauters, M., Verbeeck, H., Kasenene, J., and Boeckx, P.: Aboveground carbon stocks, woody and litter productivity along an elevational gradient in the Rwenzori Mountains, Uganda, Biotropica, https://doi.org/10.1111/btp.13114, 2022.

Pan, Y., Birdsey, R. A., Fang, J., Houghton, R., Kauppi, P. E., Kurz, W. A., Phillips, O. L., Shvidenko, A., Lewis, S. L., and Canadell, J. G.: A large and persistent carbon sink in the world's forests, Science, 333, 988-993, https://doi.org/10.1126/science.1201609, 2011.

Phillips, D. L. and Gregg, J. W.: Uncertainty in source partitioning using stable isotopes, Oecologia, 127, 171-179, https://doi.org/10.1007/s004420000578, 2001.

Quéré, C., Andrew, R. M., Friedlingstein, P., Sitch, S., Pongratz, J., Manning, A. C., Korsbakken, J. I., Peters, G. P., Canadell, J. G., and Jackson, R. B.: Global carbon budget 2018, Earth Syst. Sci. Data, 10, 405-448, https://doi.org/10.5194/essd-10-2141-2018, 2018.

R Core Team: R: A language and environment for statistical computing (R Version 4.0. 3, R Foundation for Statistical Computing, Vienna, Austria, 2020), 2021.

Rousk, J., Brookes, P. C., and Baath, E.: Contrasting soil pH effects on fungal and bacterial growth suggest functional redundancy in carbon mineralization, Applied and Environmental Microbiology, 75, 1589-1596, https://doi.org/10.1128/AEM.02775-08, 2009.

Rustad, L., Campbell, J., Marion, G., Norby, R., Mitchell, M., Hartley, A., Cornelissen, J., and Gurevitch, J.: A meta-analysis of the response of soil respiration, net nitrogen mineralization, and aboveground plant growth to experimental ecosystem warming, Oecologia, 126, 543-562, https://doi.org/10.1007/s004420000544, 2001.

Sayer, E. J. and Tanner, E. V.: A new approach to trenching experiments for measuring root–rhizosphere respiration in a lowland tropical forest, Soil Biology and Biochemistry, 42, 347-352, https://doi.org/10.1016/j.soilbio.2009.11.014, 2010.

Sayer, E. J., Heard, M. S., Grant, H. K., Marthews, T. R., and Tanner, E. V.: Soil carbon release enhanced by increased tropical forest litterfall, Nature Climate Change, 1, 304-307, https://doi.org/10.1038/nclimate1190, 2011.

Sayer, E. J., Lopez-Sangil, L., Crawford, J. A., Bréchet, L. M., Birkett, A. J., Baxendale, C., Castro, B., Rodtassana, C., Garnett, M. H., and Weiss, L.: Tropical forest soil carbon stocks do not increase despite 15 years of doubled litter inputs, Scientific reports, 9, 1-9, https://doi.org/10.1038/s41598-019-54487-2, 2019.

Schipper, L. A., Hobbs, J. K., Rutledge, S., and Arcus, V. L.: Thermodynamic theory explains the temperature optima of soil microbial processes and high Q10 values at low temperatures, Global change biology, 20, 3578-3586, https://doi.org/10.1111/gcb.12596, 2014.

Singh, B.: Soil carbon storage: modulators, mechanisms and modeling, Academic Press2018.

Walker, T. W., Kaiser, C., Strasser, F., Herbold, C. W., Leblans, N. I., Woebken, D., Janssens, I. A., Sigurdsson, B. D., and Richter, A.: Microbial temperature sensitivity and biomass change explain soil carbon loss with warming, Nature climate change, 8, 885-889, https://doi.org/10.1038/s41558-018-0259-x, 2018.

Walse, C., Berg, B., and Sverdrup, H.: Review and synthesis of experimental data on organic matter decomposition with respect to the effect of temperature, moisture, and acidity, Environmental Reviews, 6, 25-40, https://doi.org/10.1139/a98-001, 1998.

Zelles, L.: Phospholipid fatty acid profiles in selected members of soil microbial communities, Chemosphere, 35, 275-294, https://doi.org/10.1016/S0045-6535(97)00155-0, 1997.

Zeng, Z., Wang, D., Yang, L., Wu, J., Ziegler, A. D., Liu, M., Ciais, P., Searchinger, T. D., Yang, Z.-L., and Chen, D.: Deforestation-induced warming over tropical mountain regions regulated by elevation, Nature Geoscience, 14, 23-29, https://doi.org/10.1038/s41561-020-00666-0, 2021.

Zhang, W., Parker, K., Luo, Y., Wan, S., Wallace, L., and Hu, S.: Soil microbial responses to experimental warming and clipping in a tallgrass prairie, Global change biology, 11, 266-277, https://doi.org/10.1111/j.1365-2486.2005.00902.x, 2005.

Zimmermann, M., Meir, P., Bird, M. I., Malhi, Y., and Ccahuana, A.: Climate dependence of heterotrophic soil respiration from a soil-translocation experiment along a 3000 m tropical forest altitudinal gradient, European Journal of Soil Science, 60, 895-906, https://doi.org/10.1111/j.1365-2389.2009.01175.x, 2009.